

# Compact Directional Coupled-Line Coupler with Independent Power Division Ratios at Dual Bands

Siyue Zhou\*, Xiaochuan Shen, Yongle Wu, and Yuanan Liu

**Abstract**—This paper presents the first coupled-line coupler that provides independent power division ratios at dual bands. In contrast with previous dual-band coupled-line couplers, the power division ratios  $k^2(f_1)$  and  $k^2(f_2)$  at each band ( $f_1$  and  $f_2$ ) can be independently controlled in order to satisfy the requirements of various communication protocols at different bands. Moreover, it has a compact size due to the usage of coupled lines rather than transmission lines. Explicit design equations and design guide of the coupler are provided. In this letter, one prototype of the proposed coupler is simulated, fabricated, and measured. It provides power division ratios  $k^2(f_1) = 4$  dB at  $f_1 = 1$  GHz and  $k^2(f_2) = 8$  dB at  $f_2 = 2.4$  GHz. The measured result agrees well with the simulation.

## 1. INTRODUCTION

Directional couplers are one of the most critical components in modern communication systems, such as phased arrays. Among various types of couplers, the branch-line configuration shown in Fig. 1(a) is the most popular configuration, and it was invented by Levy and Lind in 1968 [1]. The core circuit of the branch-line configuration is the transmission line loop consisting of four transmission lines in the center, as drawn in solid lines in Fig. 1(a). In order to achieve advanced performances, such as dual-band operation and arbitrary power division ratio, the transmission lines inside the transmission line loop are replaced by various networks, such as  $\pi$ -networks [2, 3], T-networks [3, 4], coupled-lines [5], and transmission lines [6] as shown in Fig. 1(a). Moreover, adding extra matching networks at each port is another way to achieve advanced operations [7–10].

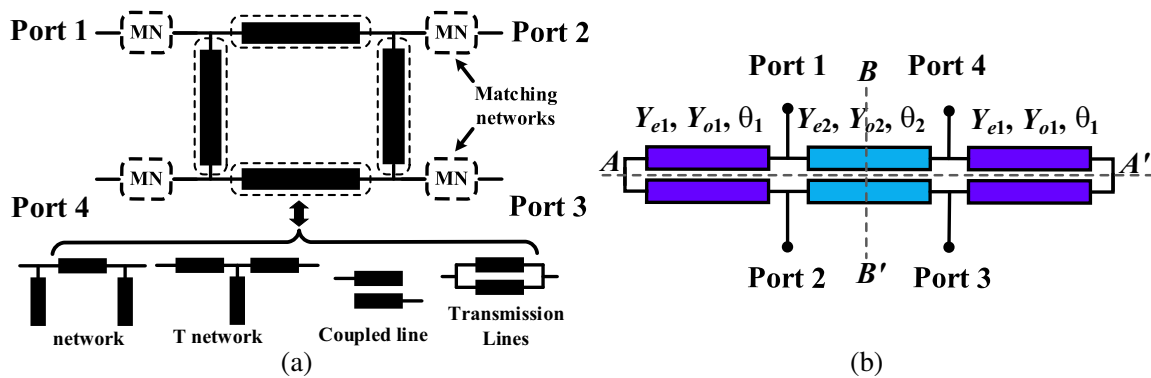


**Figure 1.** Structure of (a) branch-line configuration and (b) proposed coupled-line configuration.

Received 12 October 2019, Accepted 15 December 2019, Scheduled 26 December 2019

\* Corresponding author: Siyue Zhou (zsy.amanda@gmail.com).

The authors are with the School of Electronic Engineering, Beijing University of Posts and Telecommunications, Beijing, China.

However, the branch-line configuration suffers from large circuit size due to the wasted area inside the centered large transmission-line loop. Moreover, various networks introduced to achieve advanced operations require additional area.

In order to achieve a compact circuit size for high-level integration, the coupled-line configuration is proposed based on the structure shown in Fig. 1(b). Compact circuit size is achieved by utilizing three sections of coupled lines, avoiding the large transmission-line loop or extra matching networks. Compared with the couplers based on the branch-line configurations [1–10], the couplers based on the coupled-line configuration not only achieve compact sizes, but also provide advanced operations, such as dual-band operation [11–15], arbitrary phase-difference operation [16], and wideband performance [17].

This paper presents the first coupled-line coupler that provides an independent control of power division ratios at dual bands. Compared with dual-band coupled-line couplers with identical power division ratios ( $k^2(f_1) = k^2(f_2)$ ) at dual bands [11–17], the power division ratios of the proposed coupler can be either identical ( $k^2(f_1) = k^2(f_2)$ ) or independent ( $k^2(f_1) \neq k^2(f_2)$ ) at dual bands, which satisfies the requirements of different communication protocols at dual bands. Moreover, the general mathematical analysis of the coupled-line configuration shown in Fig. 1(b) is derived, and a detailed design guide is provided in this paper.

Although the couplers in [11] and [17] have the same structure as the proposed coupler, this paper demonstrates a more general analysis for the structure shown in Fig. 1(b) so that it can provide independent power division ratios at the dual bands, which has not been achieved by any coupled-line coupler before. The derived general analysis proves that the coupler in [11] is a special case of the proposed coupler with identical unit power division ratio ( $k^2(f_1) = k^2(f_2) = 1$ ) at dual bands and that the coupler in [17] is another special case when the coupler is treated as a single-band coupler with unit power division ratio ( $k^2 = 1$ ).

## 2. THEORY AND DESIGN

### 2.1. Single-Band Operation

Figure 1(b) depicts the schematic of the proposed dual-band directional coupler, which has a symmetrical structure and consists of three coupled lines. Specifically, even-mode characteristic admittance, odd-mode characteristic admittance, and electrical length of the coupled lines are denoted by  $y_e$ ,  $y_o$ , and  $\theta$ , respectively. Subscripts 1 and 2 are used to distinguish different coupled lines. Also, the admittance of each port is defined as  $y_0$ .

Since this coupler has two planes of symmetry ( $AA'$  and  $BB'$ ), it can be easily analyzed by utilizing even-odd mode analysis twice [1], resulting in the simplified sub-circuits shown in Fig. 2. The input admittances of the sub-circuits are shown below:

$$y_1 = j[y_{e1} \tan \theta_1 + y_{e2} \tan(\theta_2/2)] \quad (1a)$$

$$y_2 = j[-y_{o1} \cot \theta_1 + y_{o2} \tan(\theta_2/2)] \quad (1b)$$

$$y_3 = j[y_{e1} \tan \theta_1 - y_{e2} \cot(\theta_2/2)] \quad (1c)$$

$$y_4 = j[-y_{o1} \cot \theta_1 - y_{o2} \cot(\theta_2/2)] \quad (1d)$$

Then, the  $S$ -parameters of the coupler can be written as:

$$S_{11} = (\Gamma_1 + \Gamma_2 + \Gamma_3 + \Gamma_4)/4 \quad (2a)$$

$$S_{21} = (\Gamma_1 - \Gamma_2 + \Gamma_3 - \Gamma_4)/4 \quad (2b)$$

$$S_{31} = (\Gamma_1 - \Gamma_2 - \Gamma_3 + \Gamma_4)/4 \quad (2c)$$

$$S_{41} = (\Gamma_1 + \Gamma_2 - \Gamma_3 - \Gamma_4)/4 \quad (2d)$$

where  $\Gamma_i = (y_0 - y_i)/(y_0 + y_i)$ ,  $i = 1, 2, 3, 4$ .

When the port match condition ( $S_{ii} = 0$ ,  $i = 1-4$ ) and the isolation condition ( $S_{41} = 0$ ) are satisfied, the equivalent input admittances (defined as  $Y_{eq} = G_{eq} + jB_{eq}$  shown in Fig. 2(e)) of the coupler and the power division ratio (defined as  $k^2 = |S_{21}/S_{31}|^2$ ) can be expressed as:

$$G_{eq}^2 = k^2(y_1 - y_3)^2(y_2 - y_4)^2/(y_1 + y_2 - y_3 - y_4)^2 \quad (3a)$$

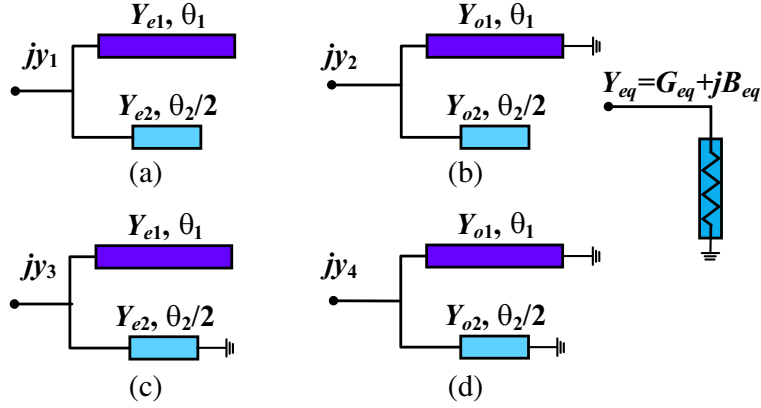


**Figure 2.** Reduced equivalent circuits of (a) even-even mode, (b) even-odd mode, (c) odd-even mode, and (d) odd-odd mode.

$$B_{eq} = (y_1 y_2 - y_3 y_4) / (y_1 + y_2 - y_3 - y_4) \quad (3b)$$

$$k^2 = (y_1 - y_4)(y_2 - y_3) / [(y_1 - y_3)(y_2 - y_4)] \quad (3c)$$

For a matching coupler,  $Y_{eq}$  should be equal to  $Y_0$ . Substituting Eq. (2) into Eq. (3) gives:

$$y_0 = 2|k| y_{e2} y_{o2} / [(y_{e2} + y_{o2}) |\sin \theta_2|] \quad (4a)$$

$$y_{e1} y_{o2} \tan \theta_1 - y_{o1} y_{e2} \cot \theta_1 - 2y_{e2} y_{o2} \cot \theta_2 = 0 \quad (4b)$$

$$k^2 = (E^2 - EF - I^2) / H - 1 \quad (4c)$$

where  $E \equiv a + b \equiv y_{e1} \tan \theta_1 + y_{o1} \tan \theta_1$ ,  $F \equiv 2(y_{e2} - y_{o2}) \cot \theta_2$ ,  $I \equiv y_{e2} - y_{o2}$ , and  $H \equiv 4y_{e2} y_{o2} / \sin^2 \theta_2$ .

If all parameters ( $y_{e1}$ ,  $y_{o1}$ ,  $\theta_1$ ,  $y_{e2}$ ,  $y_{o2}$ ,  $\theta_2$ ) satisfy the fundamental equation in Eq. (4), this coupler will have four matched ports and provide a power division ratio of  $k^2$  between outputs. Note that  $k > 0$  (or  $k < 0$ ) means that the phase of the signal at port 2 leads (or lags) the phase of the signal at port 3 by  $90^\circ$ . Note that the phase difference between outputs is always  $90^\circ$ .

The coupler reported in [17] is a special case of the proposed coupler. In [17], this coupler is discussed as a single-band coupler with a unit power division ratio between outputs ( $k^2 = 1$ ). However, this coupler can provide arbitrary power division ratio when being used as a single-band coupler according to Equation (4). Actually, Equation (8) in [17] can be derived by applying  $k = 1$  in Equation (4) in this letter. Thus, Equation (4) is a general solution with an arbitrary power division ratio, while [17] only discusses a special case when  $k = 1$ .

## 2.2. Dual-Band Implementation

As discussed above, the proposed coupler can provide an arbitrary power division ratio  $k^2$  between outputs at one certain frequency when Equation (4) is satisfied. Similarly, this coupler could provide independent power division ratios  $k^2(f_1)$  and  $k^2(f_2)$  at dual frequencies ( $f_1$  and  $f_2$ ) if Eq. (4) is satisfied simultaneously at dual bands  $f_1$  and  $f_2$ . In order to analyze dual-band performance, all parameters are regarded as functions of frequency in this section.

Using Eq. (4a) at both frequencies yields:

$$k^2(f_1) / k^2(f_2) = \sin^2 \theta_2(f_1) / \sin^2 \theta_2(f_2) \quad (5)$$

which indicates that  $\theta_2$  determines the ratio of power division ratios between dual frequencies since  $\theta_2(f_2) = \theta_2(f_1) f_2 / f_1$ . Besides,  $\theta_2$  can be calculated according to the desired power division ratios ( $k^2(f_1)$  and  $k^2(f_2)$ ) by using Eq. (5).

Assuming that  $y_{e2}$  is known,  $y_{o2}$  can be determined by Eq. (4a) as

$$y_{o2} = y_{e2} y_0 \sin \theta_2(f_i) / [2k(f_i) y_{e2} - y_0 \sin \theta_2(f_i)] \quad (6)$$

where  $i = 1$  or  $2$ . Then,  $E$ ,  $F$ ,  $I$ , and  $H$  in Eq. (4c) can be calculated since  $y_{e2}$ ,  $y_{o2}$ ,  $\theta_2$ , and  $k^2$  are known. Note that Equation (4c) is a quadratic equation, meaning that there are two solutions for  $E$  at both  $f_1$  and  $f_2$ .

$$E \equiv a + b = \left[ F \pm \sqrt{F^2 + 4I^2 + 4H(k^2 + 1)} \right] / 2 \quad (7)$$

Combining Eqs. (4b) and (7) gives the values of  $a$  and  $b$ :

$$b = y_{o2}(E - 2y_{e2} \cot \theta_2) / (y_{e2} + y_{o2}) \quad (8a)$$

$$a = E - b \quad (8b)$$

Since  $a = y_{e1} \tan \theta_1$ ,  $\theta_1$  can be obtained by Eq. (9) because  $\theta_1(f_2) = \theta_1(f_1)f_2/f_1$ .

$$a(f_1)/a(f_2) = \tan \theta_1(f_1) / \tan \theta_1(f_2) \quad (9)$$

After  $\theta_1$  is determined,  $y_{e1}$  and  $y_{o2}$  can be calculated by Eq. (8) as

$$y_{e1} = a / \tan \theta_1 \quad (10a)$$

$$y_{o1} = (E - a) / \cot \theta_1 \quad (10b)$$

In conclusion, when power division ratios at dual bands ( $k^2(f_1)$  and  $k^2(f_2)$ ) and  $y_{e2}$  are specified, all other parameters can be determined.  $\theta_1$  and  $\theta_2$  can be determined by Eqs. (5) and (9) while  $y_{e1}$ ,  $y_{o1}$ ,  $y_{o2}$  can be calculated according to Eqs. (6)–(10). Since there are four solutions of  $E$  in Eq. (7), each of  $y_{e1}$ ,  $y_{o1}$ , and  $y_{o2}$  has four possible solutions. Equation (11) can be used to screen answers because the admittance is independent of frequency.

$$y_{mn}(f_1) = y_{mn}(f_2) > 0 \quad (11)$$

where  $m = e$  or  $o$ ,  $n = 1$  or  $2$ . Note that the size of the coupler can be minimized by reducing the lengths of coupled lines by optimizing the value of  $y_{e2}$  because  $y_{e2}$  is a free parameter, and it can be optimized to achieve minimum lengths of coupled lines.

As discussed above, the proposed coupler can provide independent power division ratios at dual bands so that it must provide identical power division ratio at dual bands. When the power division ratios at both bands are identical, Equations (5)–(10) can be simplified as Eq. (12) by substituting  $k^2 \equiv k^2(f_1) = k^2(f_2)$  into Eqs. (5)–(10).

$$k^2 \equiv k^2(f_1) = k^2(f_2) \quad (12a)$$

$$\theta_1(f_1) = \theta_2(f_1) = \frac{\pi f_1}{f_1 + f_2} \quad (12b)$$

$$y_{e1} = \frac{y_{e2} \cot(\theta_1(f_1))}{\sin(\theta_2(f_1))} \left[ \sqrt{1 + \frac{4y_{e2}y_{o2}k^2}{(y_{e2} + y_{o2})^2} + \cos(\theta_2(f_1))} \right] \quad (12c)$$

$$y_{o1} = \frac{y_{o2} \tan(\theta_1(f_1))}{\sin(\theta_2(f_1))} \left[ \sqrt{1 + \frac{4y_{e2}y_{o2}k^2}{(y_{e2} + y_{o2})^2} - \cos(\theta_2(f_1))} \right] \quad (12d)$$

$$y_{o2} = y_{e2}y_0 \sin \theta_2(f_1) / [2k(f_1)y_{e2} - y_0 \sin \theta_2(f_1)] \quad (12e)$$

Equation (12) proves that all parameters can be determined when  $y_{e2}$  and  $k^2$  are specified and that the proposed coupler can provide identical power division ratios at dual bands. In this special case,  $\theta_1 = \theta_2 = 90^\circ$  at the center frequency  $f_{mid} = (f_1 + f_2)/2$ .

The dual-band coupler reported in [11] is a special case of the proposed coupler. In [11], this coupler is discussed as the dual-band coupler with identical unit power division ratios  $k^2(f_1) = k^2(f_2) = 1$ . However, Equation (12) proves that this coupler can provide arbitrary identical power division ratios at dual bands. Actually, Equations (6)–(9) in [11] can be derived by applying  $k^2(f_1) = k^2(f_2) = 1$  in Equation (12) in this letter. Therefore, Equation (12) is a general solution with arbitrary identical power division ratios at dual bands, while [11] only discusses a special case when  $k^2(f_1) = k^2(f_2) = 1$ .

In conclusion, Equations (5)–(10) demonstrate the general case that this coupler provides independent power division ratios at dual bands ( $k^2(f_1) \neq k^2(f_2)$ ). Equation (12) presents a simplified case when this coupler provides identical power division ratios at dual bands ( $k^2(f_1) = k^2(f_2)$ ).

### 2.3. Design Guide and Feasible Ranges of Power Division Ratios

As discussed in the above section, all parameters can be determined when  $k(f_1)$ ,  $k(f_2)$ , and  $y_{e2}$  are specified. A design guide for the proposed dual-band coupled-line coupler is summarized below based on Equations (5)–(11).

- Step 1, specify the required power division ratios at dual bands ( $k^2(f_1)$  and  $k^2(f_2)$ ) and the value of  $y_{e2}$ .
- Step 2, calculate  $\theta_2$  and  $y_{o2}$  according to Equations (5) and (6), respectively.
- Step 3, determine  $E$ ,  $F$ ,  $I$ , and  $H$  by Eq. (4c).
- Step 4, obtain the values of  $a$  and  $b$  by Eq. (8) based on the calculated  $E$ ,  $y_{e2}$ ,  $y_{o2}$ ,  $\theta_2$ .
- Step 5, calculate  $\theta_1$ ,  $y_{e1}$ ,  $y_{o1}$  according to Eqs. (9) and (10).
- Step 6, screen solutions for  $y_{e1}$  and  $y_{o1}$  by Eq. (11). If there are no reasonable solutions, go back to Step 1 and try new values of  $y_{e2}$ .

Based on the design guide summarized above and the analysis in Section 2.2, the feasible ranges of the power division ratios are discussed. Although the closed-form equation for each parameter cannot be directed expressed since Equations (5) and (9) are transcendental equations, numerical solutions can be calculated by using Matlab.

A Matlab code is written to find the feasible ranges of  $k(f_1)$  and  $k(f_2)$ . First, both  $k(f_1)$  and  $k(f_2)$  are swept from  $-20$  dB to  $20$  dB, which is wide enough to cover general applications. Then,  $Z_{e2}$  is swept from  $5\ \Omega$  to  $200\ \Omega$  in order to find possible solutions with given  $k(f_1)$  and  $k(f_2)$ . Moreover, different frequency ratios  $f_2/f_1$  are considered. After sweeping across all combinations of  $k(f_1)$ ,  $k(f_2)$ ,

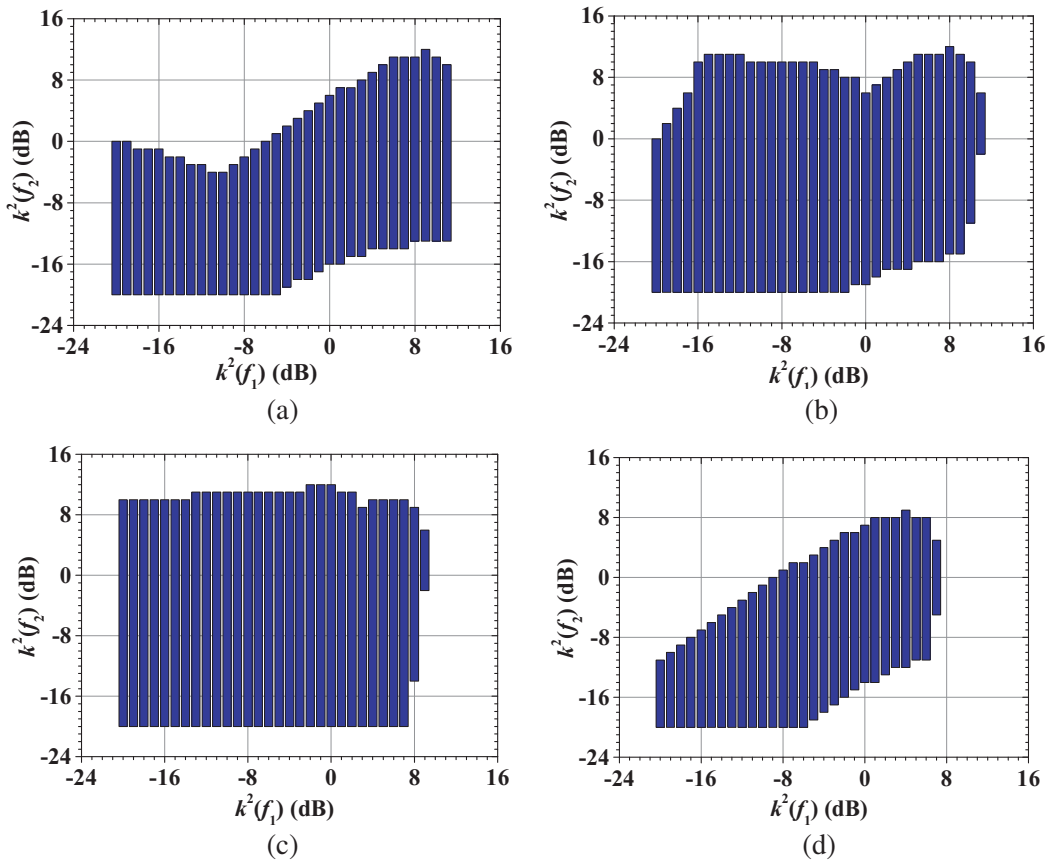


**Figure 3.** Feasible power division ratio ranges when (a)  $f_2/f_1 = 2.1$ , (b)  $f_2/f_1 = 2.4$ , (c)  $f_2/f_1 = 2.7$  and (d)  $f_2/f_1 = 3$ .

and frequency ratios  $f_2/f_1$ , the feasible ranges of  $k(f_1)$  and  $k(f_2)$  with different frequency ratios from 2.1 to 3.0 are plotted in Fig. 3. The frequency ratio ( $f_2/f_1$ ) affects the feasible ranges of  $k(f_1)$  and  $k(f_2)$ . When  $f_2/f_1 = 2.7$ , the proposed coupler can provide the widest feasible ranges of  $k(f_1)$  and  $k(f_2)$ . When the frequency ratio deviates further from 2.7, the feasible ranges of  $k(f_1)$  and  $k(f_2)$  decrease.

### 3. RESULTS AND DISCUSSION

The proposed coupler can provide independent power division ratios at dual bands within a compact size. To validate the proposed dual-band coupler, power division ratios of this coupler at dual bands are independently set:  $k^2(f_1) = 4$  dB at  $f_1 = 1$  GHz ( $|S_{21}| - |S_{31}| = 4$  dB) and  $k^2(f_2) = 8$  dB at  $f_2 = 2.4$  GHz ( $|S_{21}| - |S_{31}| = 8$  dB). This coupler is fabricated on an F4BM-2 substrate with a dielectric constant of  $\varepsilon = 2.65$  and thickness of  $h = 1$  mm. According to Eqs. (5)–(10), parameters of the coupled lines are  $Z_{e1} = 48.28 \Omega$ ,  $Z_{o1} = 44.68 \Omega$ ,  $\theta_1(f_1) = 56.37^\circ$ ,  $Z_{e2} = 135 \Omega$ ,  $Z_{o2} = 116.7 \Omega$ , and  $\theta_2(f_1) = 39.03^\circ$ . Fig. 4 shows a photograph of the fabricated coupler where  $W_1 = 3$  mm,  $S_1 = 2.9$  mm,  $L_1 = 27.58$  mm,  $W_2 = 0.4$  mm,  $S_2 = 8.9$  mm, and  $L_2 = 22$  mm.

The fabricated coupler is simulated by Advanced Design System from Keysight and measured by a VNA (Keysight E5071C). The simulated and measured  $S$ -parameters are plotted in Fig. 5. It shows that the measured frequencies of both bands slightly shift ( $f_1 = 1.03$  GHz,  $f_2 = 2.36$  GHz) due to fabrication tolerances. Return loss ( $|S_{11}|$ ) and isolation ( $|S_{41}|$ ) are both greater than 35 dB at both bands. As expected, power division ratios at dual bands are independent,  $k^2(f_1) = 3.96$  dB ( $|S_{21}| = -1.75$  dB,

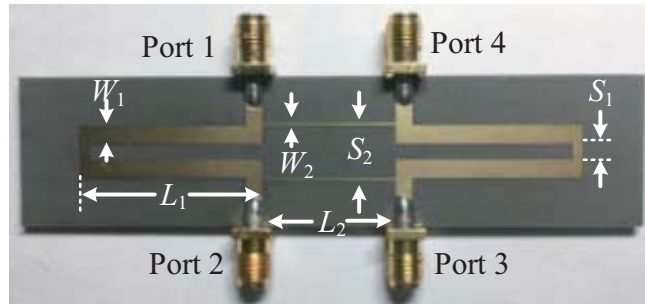


**Figure 4.** A photograph of the proposed coupler fabricated on a F4BM-2 substrate.

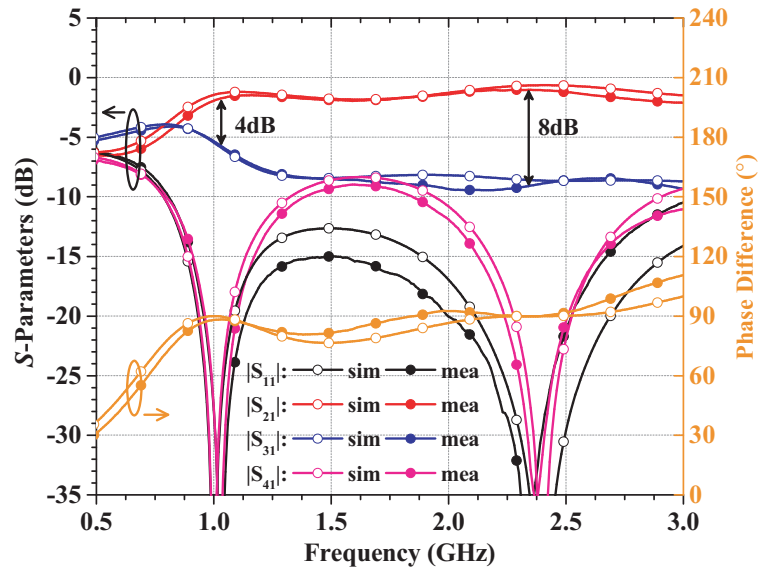


**Figure 5.** The simulated and the measured  $S$ -parameter result of proposed coupler.

$|S_{31}| = -5.71$  dB) and  $k^2(f_2) = 8$  dB ( $|S_{21}| = -1.0$  dB,  $|S_{31}| = -9.0$  dB). Also, the phase difference between the outputs is maintained at  $90^\circ$  at dual bands. The measured phase errors at each band are  $1.9^\circ$  and  $0.1^\circ$ , respectively.

A comparison table with other reported coupled-line couplers is presented in Table 1. Compared with other coupled-lined dual-band couplers, the proposed coupler is the first coupled-line coupler that provides independent power division ratios at dual bands. Moreover, the proposed coupler has the minimum size because the lengths of couple lines ( $\theta_1$  and  $\theta_2$ ) can be reduced by optimizing the free parameter  $y_{e2}$  according to the analysis in Section 2.2.

**Table 1.** Comparison against reported coupled-line couplers.

Ref.	Freq. ( $f_1/f_2$ , GHz)	Power Division Ratios ( $f_1/f_2$ , dB)	Return Loss (dB)	Isolation (dB)	BW%* ( $f_1/f_2$ )	Size
[11]	Dual-band (2/4)	Identical at dual bands, $k^2(f_1) = k^2(f_2) = 0$ dB	> 22 dB	> 24 dB	11%/5.5%	$0.252\lambda_0^2$
[12] Coupler B	Dual-band (2.4/5.8)	Identical at dual bands, $k^2(f_1) = k^2(f_2) = 10$ dB	> 25 dB	> 18 dB	22%/19.8%	$0.101\lambda_0^2$
[13] Coupler A	Dual-band 0.84, 5.17	Identical at dual bands, $k^2(f_1) = k^2(f_2) = 10$ dB	> 18 dB	> 22 dB	35%/7%	$0.023\lambda_0^2$
[14]	Dual-band (2.33/5)	Identical at dual bands, $k^2(f_1) = k^2(f_2) = 0$ dB	> 30 dB	> 30 dB	14%/17%	$0.25\lambda_0^2$
[15]	Dual-band (0.7/2.6)	Identical at dual bands, $k^2(f_1) = k^2(f_2) = 0$ dB	> 16 dB	> 16 dB	14%/14%	$0.12\lambda_0^2$
[16] Coupler A	Single-band (2)	Fixed, $k^2 = 0$ dB	> 25 dB	> 26 dB	20.6%	$0.125\lambda_0^2$
[17]	Single-band (1)	Fixed, $k^2 = 0$ dB	> 30 dB	> 25 dB	19%	$0.038\lambda_0^2$
This Work	Dual-band (1/2.4)	Independent at dual bands, $k^2(f_1) = 4$ dB, $k^2(f_2) = 10$ dB	> 35 dB	> 35 dB	12%/20.8%	$0.020\lambda_0^2$

\* The bandwidth ratio is calculated when  $|S_{11}| > 15$  dB,  $|S_{41}| > 15$  dB,  
 $k^2(f) - 1$  dB  $< ||S_{21}| - |S_{31}|| < k^2(f) + 1$  dB.

#### 4. CONCLUSION

This paper presents the first directional coupled-line coupler with independent power division ratios at dual bands. Detailed analysis of the coupled-line configuration shown in Fig. 1(b) is provided, and it proves that the reported couplers in [11] and [17] are special cases of the proposed coupler. Moreover, the design guide and feasible ranges of the power division ratios are summarized.

#### ACKNOWLEDGMENT

This work was supported by the National Natural Science Foundations of China under Grant 61821001.

#### REFERENCES

1. Levy, R. and L. F. Lind, "Synthesis of symmetrical branch-guide directional couplers," *IEEE Trans. Microw. Theory Techn.*, Vol. 16, No. 2, 80–89, Feb. 1968.

2. Zhang, H. and K. J. Chen, "A stub tapped branch-line coupler for dual-band operations," *IEEE Microw. Wireless Compon. Lett.*, Vol. 17, No. 2, 106–108, Feb. 2007.
3. Maktoomi, M. A., M. S. Hashmi, and F. M. Ghannouchi, "Systematic design technique for dual-band branch-line coupler using T- and Pi-networks and their application in novel wideband-ratio crossover," *IEEE Trans. Compon. Packag. Technol.*, Vol. 6, No. 5, 784–795, May 2016.
4. Chi, P. and K. Ho, "Design of dual-band coupler with arbitrary power division ratios and phase differences," *IEEE Trans. Microw. Theory Techn.*, Vol. 62, No. 12, 2965–2974, Dec. 2014.
5. Cheng, Y., L. Wang, J. Wu, and Y. Fan, "Directional coupler with good restraint outside the passband and its frequency agile application," *Progress In Electromagnetics Research*, Vol. 135, 759–771, 2013.
6. Gai, C., Y. Jiao, and Y. Zhao, "Compact dual-band branch-line coupler with dual transmission lines," *IEEE Microw. Wireless Compon. Lett.*, Vol. 26, No. 5, 325–327, May 2016.
7. Wu, Y., S. Y. Zheng, S. Leung, Y. Liu, and Q. Xue., "An analytical design method for a novel dual-band unequal coupler with four arbitrary terminated resistances," *IEEE Trans. Ind. Electron.*, Vol. 61, No. 10, 5509–5516, Oct. 2014.
8. Wong, Y. S., S. Y. Zheng, and W. S. Chan, "Multifolded bandwidth branch line coupler with filtering characteristic using coupled port feeding," *Progress In Electromagnetics Research*, Vol. 118, 17–35, 2011.
9. Chaudhary, G. and Y. Jeong, "Arbitrary power division ratio rat-race coupler with negative group delay characteristics," *IEEE Microw. Wireless Compon. Lett.*, Vol. 26, No. 8, 565–567, Aug. 2016.
10. Ahn, H. and M. M. Tentzeris, "Arbitrary power-division branch-line hybrids for high-performance, wideband, and selective harmonic suppressions from  $2f_0$ ," *IEEE Trans. Microw. Theory Techn.*, Vol. 67, No. 3, 978–987, Mar. 2019.
11. Yeung, L. K., "A compact dual-band 90 coupler with coupled-line sections," *IEEE Trans. Microw. Theory Techn.*, Vol. 59, No. 9, 2227–2232, Sep. 2011.
12. Wang, X., W. Yin, and K. Wu, "A dual-band coupled-line coupler with an arbitrary coupling coefficient," *IEEE Trans. Microw. Theory Techn.*, Vol. 60, No. 4, 945–951, Apr. 2012.
13. Chang, C., K. Chin, and Y. Chiang, "Dual-band coupled-line couplers with wide separation between bands," *IEEE Trans. Microw. Theory Techn.*, Vol. 65, No. 8, Aug. 2017.
14. Corrales, E., A. Baldomero, and P. Paco, "A dual-band 180-degree hybrid coupler based on coupled-line sections," *IEEE Microw. Wireless Compon. Lett.*, Vol. 25, No. 4, 211–213, Apr. 2015.
15. Chang, C., K. Chin, and Y. Zheng, "Design of dual-band  $-3$  dB couplers with a wide range of dual-band frequency ratios," *Electron. Lett.*, Vol. 52, No. 14, 1231–1233, Jul. 2016.
16. Wu, Y., J. Shen, Y. Liu, S. Leung, and Q. Xue, "Miniaturized arbitrary phase-difference couplers for arbitrary coupling coefficients," *IEEE Trans. Microw. Theory Techn.*, Vol. 61, No. 6, 2317–2324, Jun. 2013.
17. Reshma, S. and M. K. Mandal, "Miniaturization of a  $90^\circ$  hybrid coupler with improved bandwidth performance," *IEEE Microw. Wireless Compon. Lett.*, Vol. 26, No. 11, 891–893, Nov. 2016.